Ocean and Coastal Research

Original Article
Special Article Collection
Collins,C.A.; Castro,R.; Silveira,I.C.A. (Eds.)
Advances in Physical Oceanography
honoring Prof. Affonso Mascarenhas
http://dx.doi.org/10.1590/2675-2824070.22046grf
ISSN 2675-2824

Topographic solitary waves and groups

Glenn R. Flierl [1]

[1] Department of Earth, Atmospheric and Planetary Sciences (EAPS), Massachusetts Institute of Technology (MIT), Cambridge, MA 02139 USA
*Corresponding author: glenn@lake.mit.edu

Abstract

We examine nonlinear topographic waves in barotropic, rigid lid models with a focus on how depth shapes can or cannot support solitary waves. Comparisons between the full equations and the quasigeostrophic system show that the conditions for vanishing nonlinearity are different and that the transition from cyclonic to anticyclonic solitary waves does not happen for the same topographic shape. For these dynamics, however, such waves only exist for a channel geometry when the long waves can become non-dispersive. We therefore examine wave groups since short waves can have an isolated cross-topographic structure. Group solitary waves are found and analyzed with a hyperbolic tangent topography representing the transition from the shelf to deep water.

Keywords: Topographic Rossby waves, Solitary waves, Solitary groups

INTRODUCTION

Topographic Rossby waves, for which the background potential vorticity (PV) gradient is provided by the bottom slope rather than the gradient in f, have been observed in a variety of oceanic regions. On the New England continental slope, near the Gulf Stream, Thompson (1971) and Thompson & Luyten (1976) identified motions off Cape Hatteras with appropriate space and time scales, and Pickart (1995) traced these to forcing by eastward propagating meanders of the jet. Louis et al. (1982) observed them off Nova Scotia. Other locations include the Beaufort Gyre (Zhao & Timmermans 2018), the South China Sea (Shu et al. 2016, Wang et al. 2019), and east Australia (Garrett 1979). Finally, as appropriate for this collection, Oey & Lee (2002) and Hamilton (2009) found them in the Gulf of Mexico. Clarke (1971) demonstrated that the shallow water equations could have solitary and cnoidal wave solutions with a sloping bottom in a channel. A zonal shear flow could also provide the necessary potential vorticity gradient (see also (Long 1964) and (Larsen 1965)). Malanotte-Rizzoli & Hendershott (1980) and Malanotte-Rizzoli (1980), Malanotte-Rizzoli (1982) followed up on the topographic case using the quasi-geostrophic (QG) approximation.

Solitary wave packets for beta-plane waves in a channel, were studied by Yamagata (1980) again in a channel with the QG simplification. These can arise from whatever forcing creates waves in a limited region or from a modulational instability of a sinusoidal wave. Since the group velocity depends on the wavenumber and the packet has, of course, a range of wavenumbers, the envelope will deform under linear dynamics. As in the case of the solitary wave, the nonlinearity can counteract this and result

Submitted: 04-May-2022
Approved: 31-August-2022
Associate Editor: Curtis Collins

© 2022 The authors. This is an open access article distributed under the terms of the Creative Commons license.

in a packet travelling without change of form.

In this paper, we explore both kinds of nonlinear topographic Rossby waves. For the solitary waves, we examine in some detail which topographies support cyclonic or anticyclonic waves. For the wave packet, we pick a topography with a shelf, a slope, and then a flat bottom further offshore. This can support waves confined over the slope, especially when the wavelength is small.

BAROTROPIC MODEL EQUATIONS

We will use the barotropic, rigid lid, shallow water equations as the simplest model system for representing topographic Rossby waves; the rigid lid filters out the surface gravity waves. We are left with conservation of potential vorticity and a slightly more complex inversion relationship between the PV and the mass-transport streamfunction.

$$\frac{\partial}{\partial t}\mathbf{u} + (\zeta + f)\hat{\mathbf{z}} \times \mathbf{u} = -\nabla(p + \frac{1}{2}\mathbf{u}^2)$$

$$\nabla \cdot \mathbf{u}H = 0 \quad \Rightarrow \quad \mathbf{u} = \frac{H_0}{H}(-\psi_y, \psi_x)$$

We write the potential vorticity as

$$Q = H_0\frac{\zeta + f}{H} - f_0 = \frac{H_0}{H}(\zeta + f) - f_0$$

with $H_0 = H(0,0)$. The f_0 just removes a potentialy large constant.

Defining $\lambda = H_0/H$ and also $h = H/H_0$ (so we can use whichever is convenient) allows us to write the potential vorticity (PV) equation as

$$\frac{\partial}{\partial t}Q + \lambda J(\psi, Q) = 0$$

with

$$Q = \lambda\nabla \cdot \lambda\nabla\psi + \lambda f - f_0$$

It is more convenient to introduce the operator $\mathcal{L} = \nabla \cdot \lambda\nabla$ and use the vorticity equation

$$\frac{\partial}{\partial t}\zeta + J(\psi, \lambda f) + J(\psi, \lambda\zeta) = 0$$

or, written just in terms of the streamfunction,

$$\frac{\partial}{\partial t}\mathcal{L}\psi + J(\psi, \lambda f) + J(\psi, \lambda\mathcal{L}\psi) = 0 \qquad (1)$$

The quasigeostrophic (QG) version replaces λ by one in the definition of vorticity and in its advection; the second term gives the planetary and topographic beta

$$\begin{aligned} J(\psi, \lambda f) &= \lambda J(\psi, \beta y) + f J(\psi, \lambda - 1) \\ &\simeq J(\psi, \beta y) + f_0 J(\psi, \lambda - 1) \end{aligned}$$

The QGPV is then

$$Q_{qg} = \nabla^2\psi + \beta y + f_0(\lambda - 1)$$

and satisfies

$$\frac{\partial}{\partial t}Q_{qg} + J(\psi, Q_{qg}) = 0 \qquad (2)$$

If $\lambda - 1$ is, as required, small (order $\delta H/H_0$), then we expand and drop all higher order terms. If we write the QG system in terms of the topographic elevation $B(\mathbf{x}) = H_0 - H(\mathbf{x})$, λ becomes $(1 - B/H_0)^{-1}$ and the QG topographic beta is just $f_0 B(\mathbf{x})/H_0$ (dropping terms higher order in B/H_0). The QGPV takes the familiar form

$$Q_{qg} = \nabla^2\psi + \beta y + f_0\frac{B}{H_0}$$

We will use $H = H(y)$ for the rest of the paper.

Linear but also nonlinear solutions

Just as a single Rossby wave in the beta-plane barotropic vorticity equation is a nonlinear solution, we can ask when that also holds in the full equation (1). A steadily propagating solution will have

$$\frac{\partial}{\partial t}Q = -c\frac{\partial}{\partial x}Q = \lambda J(c\int^y h, Q) \equiv \lambda J(\psi + cR, Q)$$

with $R = \int^y h$. We let

$$\mathcal{Q}(\phi) = -K^2\phi$$

so that

$$\nabla \cdot \lambda\nabla\psi + f - f_0 h = -K^2 h\psi - cK^2 hR$$

The x-dependent and x-independent parts must balance separately

$$\nabla \cdot \frac{1}{h}\nabla\psi = -K^2 h\psi$$

so that K^2 is a total wavenumber, while

$$\frac{f}{h} - f_0 = f\lambda - f_0 = -cK^2 R$$

relates the propagation speed to the topography and the wavenumber. Taking a y-derivative gives

$$\frac{\partial}{\partial y}(f\lambda) = -cK^2 h = -cK^2 \frac{f}{f\lambda}$$

so that the linear solution will satisfy the nonlinear equations when the topography has the form

$$f\lambda \frac{\partial}{\partial y}(f\lambda) = f_0 f \alpha$$

with α a constant. The dispersion relation is simply

$$c = -\frac{\alpha f_0}{K^2}$$

Solving the equation for the topography gives

$$f\lambda = \sqrt{f_0^2 + 2\alpha f_0^2 y + \alpha f_0 \beta y^2}$$

(with the condition $\lambda(0) = 1$). In terms of the depth, the topography must satisfy

$$\frac{H}{H_0} = h = \frac{1 + \beta y / f_0}{\sqrt{1 + 2\alpha(y + \beta y^2 / 2 f_0)}}$$

On the f-plane, this says our topography is

$$h = (1 + 2\alpha y)^{-1/2} \quad or \quad \lambda = (1 + 2\alpha y)^{1/2}$$

Thus we have related the wave speed to the shape and slope of the topography. In particular, if the bottom elevation is

$$\begin{aligned} &B = H_0 - H = H_0(1 - h) \\ &\quad and \\ &s = \frac{\partial}{\partial y} B = -H_0 \alpha (1 + 2\alpha y)^{-3/2} \quad \Rightarrow \\ &s(0) = H_0 \alpha \end{aligned}$$

we find

$$c = -\frac{f_0 s(0)}{H_0} \frac{1}{K^2}$$

This is exactly the QG result, but here the slope is not constant, and the structure of the wave is not sinusoidal in y. Note that this can only work in a bounded region, since H will blow up for $y = -1/(2\alpha)$. Therefore, we need at least one wall at some y north of this point.

Solitary waves

For the rest of the paper, we will ignore the planetary β; the y direction is now upslope and the x is along the topography. The equations will be nondimensionalized with the time scale $1/f_0$ and space scale L characterizing the slope ($\frac{\partial H}{\partial y} \sim H_0/L$). The equations become

$$\begin{aligned} &\frac{\partial}{\partial t}\zeta + \beta \frac{\partial}{\partial x}\psi + J(\psi, \lambda\zeta) = 0 \\ &\zeta = \nabla \cdot \lambda \nabla \psi \quad , \quad \beta = \frac{\partial}{\partial y}\lambda \end{aligned}$$

with the QG form having $\lambda \to 1$ and retaining only the lowest order term in the expansion of the topographic β.

Clarke (1971) derived the solitary wave solutions like those here; we are adding the KdV equation and more discussion on the role of the topographic form on the waves. Malanotte-Rizzoli & Hendershott (1980) also studied the dynamics, but using the quasi-geostrophic equations; qualitatively, these are similar to the cases here with order one variation in amplitude, but there are noticeable quantitative differences.

If there are no closed streamlines in the co-moving frame, then we just have

$$\nabla \cdot \frac{1}{h} \nabla \psi = h\mathcal{Q}\left(R + \frac{\psi}{c}\right) - h\mathcal{Q}(R)$$

For velocities small compared with the phase speed, we can Taylor-expand the r.h.s.

$$\nabla \cdot \frac{1}{h} \nabla \psi = \frac{1}{c} h\mathcal{Q}' \psi + \frac{1}{2c^2} h\mathcal{Q}'' \psi^2$$

and evaluate the $\mathcal{Q}'$ by y-derivatives of

$$\mathcal{Q}\left(\int_0^y h\right) = \frac{1}{h} - 1 = (\lambda - 1)$$

giving

$$h\mathcal{Q}' = \frac{\partial}{\partial y}\lambda \equiv \beta(y) \quad and \quad h\mathcal{Q}'' = \frac{1}{2}\frac{\partial^2}{\partial y^2}\lambda^2 \equiv \gamma(y)$$

If h decreases monotonically towards positive y then λ increases with y. (In the limit of small depth variations λ is nearly equal to a constant plus the topography height divided by H_0.)

With these definitions, our Taylor-expanded

equation[1], is

$$\nabla \cdot \lambda \nabla \psi = \frac{\beta}{c}\psi + \frac{\gamma}{2c^2}\psi^2 \tag{3}$$

Although the steps below can be taken in general, we note that there is a particular topography for which the Taylor-series truncates exactly; i.e., $\mathcal{Q}$ is a quadratic function of its argument:

$$\mathcal{Q}(\phi) = \left(\frac{a}{3}\phi + 1\right)^2 - 1 \quad \Rightarrow \quad h = (1 + ay)^{-2/3}$$

In that case, which we will call "quadratic topography", the wave satisfies (3) exactly with

$$\beta = \frac{2a}{3}h^{1/2} \quad , \quad \gamma = \frac{2a^2}{9}h$$

There is no restriction on the amplitude; when, however, there are closed streamlines, $\mathcal{Q}$ need not be the same on interior streamlines as it is on the ones extending to infinity. This does not mean that the solution is invalid, but rather that there are many other solutions with different $\mathcal{Q}(R + \psi/c)$ interior functions. Examples of such multi-valued $\mathcal{Q}$ functions are "modons" (Stern 1975, Flierl et al. 1980) and potential vorticity patches (Moore & Saffman 1971); cases with topography include Wang (1992), Baker-Yeboah et al. (2010) Zhang et al. (2011).

We just summarize Clarke's (1971) procedure: look for an approximate solution of the form

$$\psi = \epsilon^2 A(\epsilon x) g(y) + \epsilon^4 \psi_1$$

At the lowest order

$$\mathcal{D}_0(g) \equiv \frac{\partial}{\partial y}\lambda\frac{\partial}{\partial y}g = \frac{\beta}{c_0}g \tag{4}$$

This determines the meridional structure and, with appropriate boundary conditions, the lowest order phase speed c_0.

The second order equation is

$$\mathcal{D}_0(\psi_1) - \frac{\beta}{c_0}\psi_1 + g\lambda\frac{\partial^2}{\partial x^2}A = -\frac{c_1\beta g}{c_0^2}A + \frac{\gamma g^2}{2c_0^2}A^2$$

We multiply by g and integrate (with the integral notated as $\langle \bullet \rangle$), using the fact that the operator $\mathcal{D}_0 - \beta/c_0$ is self-adjoint. The result is

$$\langle \lambda g^2 \rangle \frac{\partial^2}{\partial x^2}A = -A\frac{c_1}{c_0^2}\langle g^2\beta\rangle + \frac{\langle g^3\gamma\rangle}{2c_0^2}A^2$$

For an isolated disturbance A_{xx} will have the same sign as A so that we can have decaying exponentials when A is small. Taking into account $\mathcal{Q}' > 0 \Rightarrow \beta > 0$, this condition requires $c_1 < 0$. As is characteristic of solitary waves, it will travel faster than the fastest long wave. (This is implicit in the QG dispersion relation $c = c_0/(1 + k^2/\ell^2)$ but with k^2 negative.) To match between the decaying solutions to the right and left, there must be a region where the amplitude is large enough so that the second term dominates and makes the second derivative of A be opposite in sign from A. This requires $A\langle g^2\gamma\rangle < 0$ where g is the gravest mode across the channel and is chosen to be positive. If h^{-2} has positive [negative] curvature, the eddy will be cyclonic [anticyclonic].

The usual solution for the x-structure of the wave

$$\begin{aligned} A \quad & A_0 \operatorname{sech}^2(Kx) \\ & with \\ c_1 \quad = \quad & -4K^2c_0^2\frac{\langle \lambda g^2\rangle}{\langle \beta g^2\rangle} \\ A_0 \quad = \quad & -12K^2c_0^2\frac{\langle \lambda g^2\rangle}{\langle \gamma g^3\rangle} \end{aligned}$$

indeed shows that $c_1 < 0$ and, for positive γ, that the wave is cyclonic with a low in the streamfunction, $A_0 < 0$.

KdV

To demonstrate that these are "solitons", we shall show that the time-dependent equation for the amplitude is indeed the Kortweg-deVries equation, so that faster eddies will pass through slower ones with only a phase shift, and arbitrary, localized disturbance of the right sign will break up into a set of solitons and a weak dispersive field. See the literature on "inverse scattering", e.g., Ablowitz & Segur (1981).

In the vorticity equation

$$\frac{\partial}{\partial t}\zeta + J(\psi, \lambda) + J(\psi, \lambda\zeta) = 0$$

[1]The QG form will be the same except $\zeta = \nabla^2\psi$ and $\gamma = \partial^2\lambda/\partial y^2$; for the sample topographies in table 1, the values can be quite different from our finite-topography case

with

$$\zeta = \zeta(x - c_0 t, y, t) \quad \Rightarrow$$
$$\frac{\partial}{\partial t}\zeta + \frac{\partial}{\partial x}(\psi\beta - c_0\zeta) + J(\psi, \lambda\zeta) = 0$$

we introduce a long scale for x, a slow time, and small amplitude waves

$$\zeta = \epsilon\zeta(\epsilon x, y, \epsilon^2 t) \quad , \quad \zeta = \mathcal{D}_0\psi + \epsilon^2\lambda\frac{\partial^2\psi}{\partial x^2}$$

The order ϵ equation is just

$$\frac{\partial}{\partial x}(\psi_0\beta - c_0\mathcal{D}_0\psi_0) = 0$$

which has the solution

$$\psi_0 = A(\epsilon x, \epsilon^2 t)g(y)$$

The translation rate c_0 is the long wave speed – the gravest eigenvalue of

$$\mathcal{D}_0 g = \frac{g}{c_0}\beta(y) \quad with \quad g(y_0) = g(y_1) = 0$$

The order ϵ^3 equation includes the order ϵ^2 correction to ψ_0 and terms with the large-scale derivatives in x and t

$$\frac{\partial A}{\partial t}\mathcal{D}_0 g \quad + \quad \frac{\partial}{\partial x}(\psi_1\beta - c_0 D\psi_1) - c_0\lambda\frac{\partial^3 A}{\partial x^3}g$$
$$+ \quad A\frac{\partial A}{\partial x}\left(g\frac{\partial}{\partial y}\lambda Dg - \frac{\partial g}{\partial y}\lambda Dg\right) = 0$$

Multiplying by g and integrating over y gives

$$\frac{\langle\beta g^2\rangle}{c_0}\frac{\partial A}{\partial t} - c_0\frac{\partial^3 A}{\partial x^3}\langle\lambda g\rangle$$
$$+ A\frac{\partial A}{\partial x}\langle g^2\frac{\partial}{\partial y}\lambda Dg - g\frac{\partial g}{\partial y}\lambda Dg\rangle = 0$$

Substituting $\mathcal{D}_0 g = g\beta/c_0$ leads to

$$\frac{\partial A}{\partial t} - c_0^2\frac{\langle\lambda g^2\rangle}{\langle\beta g^2\rangle}\frac{\partial^3 A}{\partial x^3} + A\frac{\partial A}{\partial x}\frac{\langle\gamma g^3\rangle}{\langle\beta g^2\rangle} = 0$$

This is a form of the KdV equation; therefore the long waves will indeed behave like solitons as long as they all have the same y-structure.

Topographic shape

The shape used for the topography determines the sign of the solitary waves; however, some choices can also be convenient in that the lowest order equation for the y-structure has a simple form. Fig. 1 shows sample plots of the depth profiles, with characteristic properties listed in table 1. The case

$$h = \frac{1}{(1+ay)^n} \quad or \quad \lambda = (1+ay)^n$$

gives a simple expression for $\gamma = a^2 n(2n-1)(1+ay)^{2n-2}$ showing that it will be negative for $0 < n < 0.5$ (anticyclones) and positive for $n > 0.5$ (cyclones). The latter includes our quadratic topography with $n = 2/3$. The $n = 1/2$ case, not surprisingly, has $\gamma = 0$ so that nonlinear steepening cannot balance dispersion. The $n = 1/4$ topography, which supports anticyclones has a long, fairly flat shelf with a rapid drop-off (Fig. 1). The linear slope, $n = 1$, used in QG models as an equivalent β no longer has $\gamma = 0$ so that nonlinear effects will enter at long times.

For $\psi = \lambda^{-1/2}\phi$, the vorticity operator becomes

$$\zeta = \lambda^{1/2}\left[\nabla^2 - \lambda^{-1/2}\frac{\partial^2\lambda^{1/2}}{\partial y^2}\right]\phi$$

and our steadily-propagating equation becomes

$$\left[\nabla^2 - \frac{1}{\lambda^{1/2}}\frac{\partial^2\lambda^{1/2}}{\partial y^2}\right]\phi = \frac{\beta}{\lambda c}\phi + \frac{\gamma}{2c^2\lambda^{3/2}}\phi^2$$

The north-south structure equation with $g = \lambda^{-1/2}G(y)$ is

$$\frac{\partial^2}{\partial y^2}G - \Gamma G = \frac{1}{c_0}\frac{\beta}{\lambda}G \quad with \quad \Gamma = \frac{1}{\lambda^{1/2}}\frac{\partial^2\lambda^{1/2}}{\partial y^2}$$

In table 2, we use this to present forms of the topography which will have analytical solutions for G in the domain $1/2 \le y \le 1/2$.

The values of B and k will be set by the positions of the walls such that G vanishes. We will have $c < 0$ so that k is real. Special cases of the Bessel functions are included in the table. Higher order Bessel function or spherical Bessel function solutions will exist for integer or half integer n values, respectively. The sign of k also has to be chosen so that the solutions are oscillatory in the domain; for the Airy functions we need $kz^{1/2} < 0$ so that the minus sign is required.

Two-D solitary waves

The solitary wave solutions are not entirely satisfactory; one would like to consider a topography which,

Table 1. Example profiles

λ		β	γ
$\exp(ay)$		$a\exp(ay)$	$2a^2\exp(2ay)$
$(1+ay)^n$		$na(1+ay)^{n-1}$	$n(2n-1)a^2(1+ay)^{2n-2}$
$(1+ay)$		a	a^2
$(1+ay)^{1/2}$		$\frac{1}{2}a(1+ay)^{-1/2}$	0
$(1+ay)^{2/3}$		$(2/3)a(1+ay)^{-1/3}$	$(2/9)a^2(1+ay)^{-2/3}$
$(1-a'y)^{-1}$	$(n=-1,\ a=-a')$	$a'(1-a'y)^{-2}$	$3a'^2(1-a'y)^{-4}$

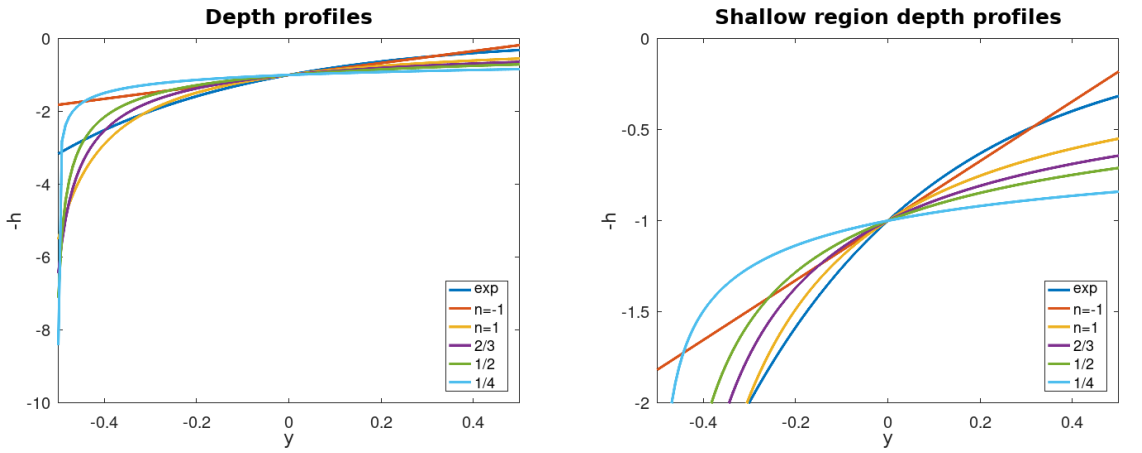

Figure 1. Depth profiles $-h(y)$ for $\lambda = e^{ay}$ and $(1+ay)^n$ with $n = 1,\ 2/3$ (cyc.), $1/2$ (no solitary waves), $1/4$ (anticyc.). The corresponding values of $\gamma(0)/a^2$ are $2,\ 1,\ 2/9, 0, -1/8$. a is chosen so that the depth range is $10H_0$ in the interval $-1/2 < y < 1/2$. The $n = -1$ case corresponds to a constant slope and has $a = -18/11$ with $\gamma/a^2 = 3$ (cyc.).

Table 2. Topography with analytic solutions

λ	Γ	$\beta\lambda^{-1}$	$\gamma\lambda^{-3/2}$
$\exp(ay)$	$a^2/4$	a	$2a^2\exp(ay/2)$
$(1+ay)^n$	$\frac{a^2}{4}n(n-2)(1+ay)^2$	$na(1+ay)^{-1}$	$n(2n-1)a^2(1+ay)^{n/2-2}$
$(1-ay)^{-1}$	$(3/4)a^2(1-ay)^{-2}$	$a(1-ay)^{-1}$	$3a^2(1-ay)^{-5/2}$
λ	G	notes	c_0
$\exp(-ay)$	$\cos(\pi y)$		$-a/(\pi^2+a^2/4)$
$(1+ay)^n$	$z^{1/2}\mathcal{C}_\nu(kz^{1/2}) + Bz^{1/2}\mathcal{C}_{-\nu}(kz^{1/2})$ (Bessel functions)	$z = (1+ay) > 0$, $\nu = \lvert 1-n\rvert$, $k = \pm\sqrt{-4n/ac_0}$	
n (Bessel cases)	ν	functions $\mathcal{C}_{\pm\nu}$	
-1, $a<0$	2	ordinary Bessel functions J_2, Y_2	
0	1	J_1, Y_1	
1/2	1/2	spherical Bessel functions j_0, y_0	
2/3	1/3	Airy functions Ai, Bi	
1	0	J_0, Y_0	

like the continental slope, has a limited extent connecting two flat regions. But using a representative topographic model $\lambda = 1 + d\tanh(y)$ indicates the problem. The solutions in the flat regions just have $\partial^2\psi/\partial y^2 = 0$ so that solutions will not decay. Indeed, if we look at the QG form, the y-structure problem

$$\frac{\partial^2 g}{\partial y^2} = \frac{d\,\mathrm{sech}^2(y)}{Lc}g$$

has one solution $g = \tanh(y)$ with $c = -d/2$. The second solution is linear in y away from the topography

$$g = e^y \mathrm{sech}(y) - (y+1)\tanh(y)$$

While this suggests we need a two-scale approach with y-variation on scales comparable to the length of the solitary wave, we suspect this will still not lead to solutions. The difficulty is that the linear wave solutions which are bounded in y are not non-dispersive in the long wave limit, but, as shown in the next section, have $c \sim -d/k$. So the standard approach of starting with a large scale structure with weak dispersion and weak nonlinearity will not work.

Large amplitude solitons can have closed streamlines, in which case $\mathcal{Q}(R+\psi/c)$ is not determined by the value on the open streamlines. Adding PV anomalies in the interior may give solutions which decay in the flat areas (as would a point vortex), but would not prevent loss of energy by radiation since the speed would still resonate with some waves; c.f, Flierl & Haines (1994).

However, we can expect there will be isolated dipole solutions ("modons") moving eastward. This is apparent if we take d small so that we can use QG and an examine a dipole centered at $y = 0$ with small enough scale that $\lambda - 1 \simeq dy$. The modons in the barotropic vorticity equation (Larichev & Reznik 1976, Flierl et al. 1980) will be good approximations to solutions.

ENVELOPE SOLITARY WAVES

We will use the hyperbolic tangent inverse topography which has a sloping bottom joining a shallow shelf to the deep ocean

$$\begin{aligned} \lambda &= 1 + d\tanh(y) \quad \Rightarrow \\ \beta &= d\,\mathrm{sech}^2(y) \\ \gamma &= d\,\mathrm{sech}^2(y)[3d\,\mathrm{sech}^2(y) - 2\tanh(y) - 2d] \end{aligned}$$

as shown in Fig. 2. We will be using a multi-scale expansion of the basic equation

$$\frac{\partial}{\partial t}\mathcal{L}\psi + \beta\frac{\partial}{\partial x}\psi + J(\psi, \lambda\mathcal{L}\psi) = 0$$

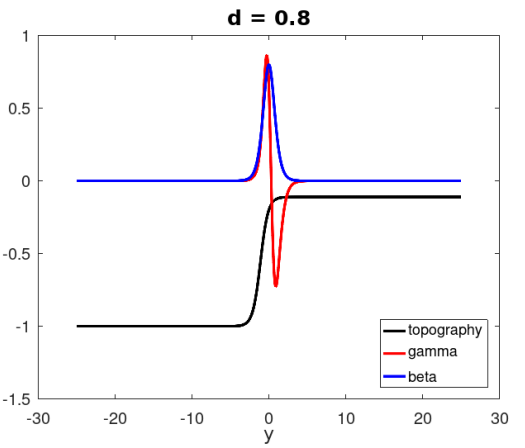

Figure 2. Characteristics of the shelf-slope topography for $\lambda = H(0)/H = 1 + d\tanh(y)$. The bathymetry is shown as $-H(y)/H(-\infty)$.

assuming the packet is long in the x-direction compared to the carrier wave and that the amplitude is small.

Linear solution

The linear problem has solutions

$$\psi = Ae^{ik(x-ct)}g(y) + c.c.$$

The y-structure is defined by the eigenvectors of

$$\mathcal{D}_1 g \equiv \left[\frac{\partial}{\partial y}\lambda\frac{\partial}{\partial y} - \lambda k^2\right] g = \frac{\beta}{c} g \qquad (5)$$

The operator $\mathcal{D}_1$ and its relatives

$$\mathcal{D}_n = \frac{\partial}{\partial y}\lambda\frac{\partial}{\partial y} - \lambda n^2 k^2$$

will appear in solving for the harmonics of the carrier wave. (We have already seen $\mathcal{D}_0$ in section 3.)

The QG form simply replaces λ with 1; the solutions are

$$g(y) = \mathrm{sech}^k(y) \quad , \quad c = -\frac{d}{k^2 + k}$$

[dimensionally, $c = -(df/L)/(k^2 + k/L)$ with L the topographic width and df/L acting as β]. The eigenfunctions $g(y)$ of the full (non-QG) equation (4), found numerically, are not symmetrical, being peaked in slightly deeper water and showing a more rapid decay offshore than onshore (Fig. 3). This is most noticeable when the ratio of the shelf and offshore depths $(1-d)/(1+d)$ is small. This

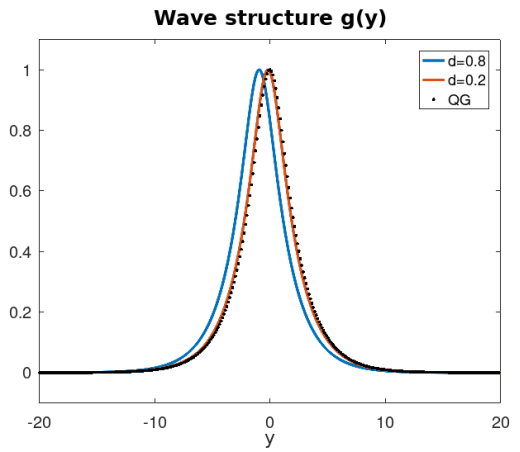

Figure 3. $g(y)$ for $k = 0.5$ and $d = 0.2$ or 0.8 for the full equations and the QG approximation.

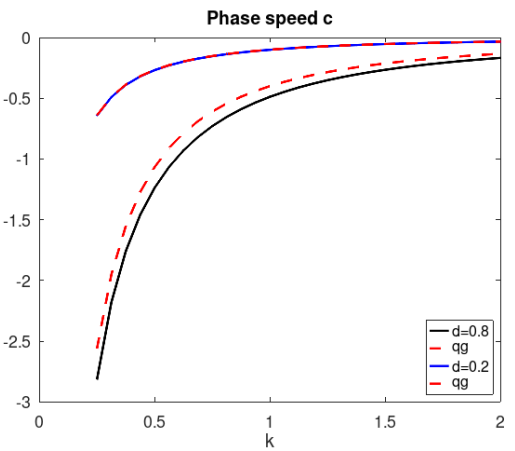

Figure 4. $c(k)$ $d = 0.2$ and 0.8 for the full equations and the QG approximation (dashed).

suggests that QG may be acceptable, given the simplifications aleady in the setup: the neglect of stratification and variations in slope and orientation of the topography. However, we will continue to use numerics.

The phase speed, c, is also quite simlar to the QG result (Fig. 4); like β-plane Rossby waves, these move westward, and the speed decays as $1/k^2$ for short waves. Long waves, however, have a cross-topography structure which widens with the wavelength, so that the average topographic β decreases and $c \sim -1/k$.

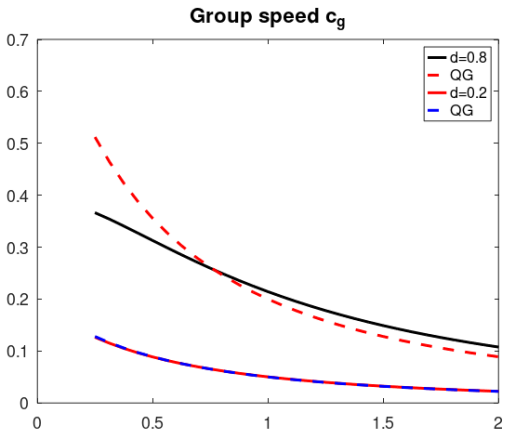

Figure 5. $c_g(k)$ $d = 0.2$ and 0.8 for the full equations and the QG approximation (dashed).

Wave packets

A packet will travel at the group velocity; this is eastward and varies with the primary wavenumber (Fig. 5).

But the envelope itself will change with time under linear dynamics since the packet has a peaked spectrum, and the different waves have slightly different c_g values. This evolution occurs on a time-scale on the order of the time scale for the waves $(1/\omega)$ times the square of the ratio of packet to carrier wave scale.

The nonlinearity can enter in several ways: the linear solution does not exactly satisfy the nonlinear equations:

$$\begin{aligned} J(\psi, \lambda\mathcal{L}\psi) = J(\psi, \frac{\beta\lambda}{c}\psi) &= \psi\frac{\partial\psi}{\partial x}\frac{\partial}{\partial y}(\beta\lambda) \\ &= \frac{1}{2}\gamma(y)\frac{\partial}{\partial x}\psi^2 \neq 0 \end{aligned}$$

and this term will generate both harmonics and a packet-scale flow. These interact with the primary wave to alter the group propagation speed and its shape.

In the multi-scale approach, we define ϵ to be the ratio of the carrier wave scale to the packet width; then the streamfunction can be written as

$$\psi \to \epsilon\psi(x - ct, \epsilon(x - c_g t), \epsilon^2 t) \to \epsilon\psi(x, X, T)$$

and the various derivatives become

$$\frac{\partial}{\partial t} \to -c\frac{\partial}{\partial x} - \epsilon c_g\frac{\partial}{\partial X} + \epsilon^2\frac{\partial}{\partial T} \quad , \quad \frac{\partial}{\partial x} \to \frac{\partial}{\partial x} + \epsilon\frac{\partial}{\partial X}$$

with the $\to$ indicating that these replacements are

used in our dynamical equation (1) (divided by ϵ). Then ψ is expanded in powers of ϵ, and we end up with a sequence of equations

$$\begin{aligned}
-c\frac{\partial}{\partial x}\mathcal{L}_0\psi_0+\beta\frac{\partial}{\partial x}\psi_0 &= 0 && (6)\\
-c\frac{\partial}{\partial x}\mathcal{L}_0\psi_1+\beta\frac{\partial}{\partial x}\psi_1 &= c_g\frac{\partial}{\partial X}\mathcal{L}_0\psi_0-\beta\frac{\partial}{\partial X}\psi_0\\
+c\frac{\partial}{\partial x}\mathcal{L}_1\psi_0 &- J(\psi_0,\lambda\mathcal{L}_0\psi_0) && (7)\\
-c\frac{\partial}{\partial x}\mathcal{L}_0\psi_2+\beta\frac{\partial}{\partial x}\psi_2 &= c_g\frac{\partial}{\partial X}\mathcal{L}_1\psi_0+c_g\frac{\partial}{\partial X}\mathcal{L}_0\psi_1\\
-\beta\frac{\partial}{\partial X}\psi_1 &+ c\frac{\partial}{\partial x}\mathcal{L}_2\psi_0+c\frac{\partial}{\partial x}\mathcal{L}_1\psi_1\\
-\frac{\partial}{\partial T}\mathcal{L}_0\psi_0 &- J_X(\psi_0,\lambda\mathcal{L}_0\psi_0)\\
-J(\psi_0,\lambda\mathcal{L}_1\psi_0) &- J(\psi_1,\lambda\mathcal{L}_0\psi_0)\\
&- -J(\psi_0,\lambda\mathcal{L}_0\psi_1) && (8)
\end{aligned}$$

with the definitions

$$\mathcal{L}_0=\nabla\cdot\lambda\nabla \quad , \quad \mathcal{L}_1=2\lambda\frac{\partial^2}{\partial x\partial X} \quad , \quad \mathcal{L}_2=\lambda\frac{\partial^2}{\partial X^2}$$

$$J(a,b)=a_xb_y-a_yb_x \quad , \quad J_X(a,b)=a_Xb_y-a_yb_X$$

ZEROTH ORDER: Equation (6) has the linear solution but with a spatially and temporarily varying amplitude

$$\psi_0=A(X,T)\,e^{\imath k[x-ct]}g(y)+c.c.$$

resulting in the eigenvalue/eigenfunction equation above (5) and the characteristics portrayed in Fig. 6.

FIRST ORDER: The solvability equation, formed by multiplying (7) by the adjoint solution $\exp(-\imath kx)g(y)$, averaging over x, and integrating over y, eliminates the left side.[2] From the right side, we have

$$\frac{\partial A}{\partial X}\left[\frac{c_g}{c}\langle\beta g^2\rangle-\langle\beta g^2\rangle-2ck^2\langle\lambda g^2\rangle\right]=0 \quad\Rightarrow$$
$$c_g=c+2c^2k^2\frac{\langle\lambda g^2\rangle}{\langle\beta g^2\rangle}$$

with $\langle F\rangle=\int_{-\infty}^{\infty}F(y)dy$. We can verify that the group velocity matches the usual definition

$$c_g=\frac{\partial}{\partial k}kc=c+k\frac{\partial c}{\partial k}$$

[2]Which is a solution to the zeroth order problem since $-c\mathcal{L}_0+\beta$ is self-adjoint.

by differentiating the equation (5) for the dispersion relation with respect to k

$$\begin{aligned}
[c\mathcal{D}_1-\beta]\frac{\partial g}{\partial k} &= -\left[\frac{\partial c}{\partial k}\mathcal{D}_1g-2c\lambda kg\right]\\
&= -\left[\frac{1}{c}\frac{\partial c}{\partial k}\beta g-2c\lambda kg\right]
\end{aligned}$$

Again, projecting with g leads to

$$\frac{\partial c}{\partial k}\langle\beta g^2\rangle=2c^2k\langle\lambda g^2\rangle$$

which is consistent with the expression above. Note that, as expected from the dispersion relation figure, the group velocity is positive so that the packet propagates in the opposite direction as the peaks and troughs.

The first order stream function takes the form

$$\begin{aligned}
\psi_1 &= A_0(X,T)g_0(y)+A_1(X,T)e^{\imath kx}g_1(y)+c.c.\\
&+ A_2(X,T)e^{\imath 2kx}g_2(y)+c.c.
\end{aligned}$$

The Jacobian, $J(\psi_0,\lambda\mathcal{L}_0\psi_0)$ gives only second harmonic terms; these lead to

$$A_2=\frac{1}{2c^2}A^2 \quad , \quad \left[\mathcal{D}_2-\frac{\beta}{c}\right]g_2=\gamma g^2 \qquad (9)$$

The A_1 term arises because there is a non-resonant residual after substituting the expression for c_g in the linear terms; this gives

$$A_1=\frac{\imath}{kc}A_X \quad , \quad \left[\mathcal{D}_1-\frac{\beta}{c}\right]g_1=\left[\frac{c_g}{c}\beta-\beta-2ck^2\lambda\right]g \qquad (10)$$

Finally the A_0, which is the packet-scale flow, represents an x-independent solution to the left side. Its amplitude and structure comes from the next order.

SECOND ORDER: The right side of (8) will have terms which do not depend on x; these produce an equation for A_0g_0:

$$\begin{aligned}
A_0 &= |A|^2\\
(c_g\mathcal{D}_0-\beta)g_0 &= \frac{\gamma}{c}g^2-\frac{1}{c^2}\frac{\partial}{\partial y}(\beta\lambda gg_1)\\
&+ \frac{1}{c}\frac{\partial}{\partial y}(g\lambda\mathcal{D}_1g_1)+k^2\frac{\partial}{\partial y}(\lambda^2g^2)
\end{aligned}$$

We again project (8) by the adjoint to end up with

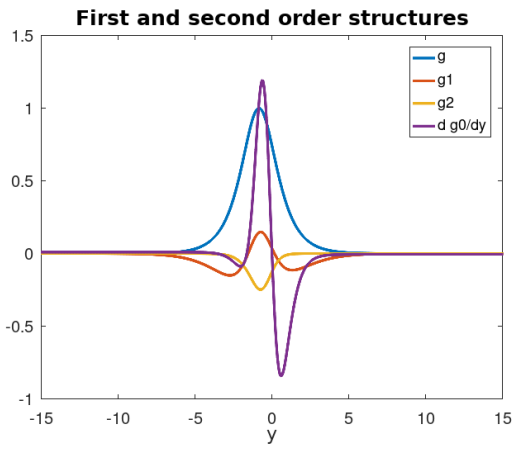

Figure 6. y-structures g, g_1, g_2, $\partial g_0/\partial y$ for $k = 1$. The function g_0 limits to linear slopes, positive (negative) for $y << 0$, $y >>: 0$. We plot the $\partial g_0/\partial y$ because that's all that enters into the coefficients below.

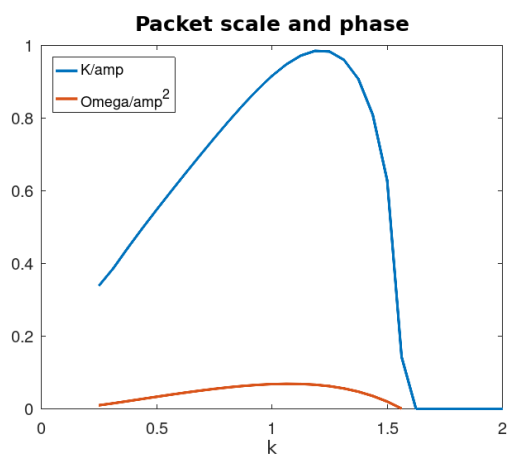

Figure 7. Amplitude-dependent packet $K/\mathcal{A} = \sqrt{f_3/2f_2}$ setting the inverse size and $\Omega/\mathcal{A}^2$ setting the frequency shift.

the equation satisfied by the envelope

$$f_1 A_T + \imath k f_2 A_{XX} + \imath k f_3 |A|^2 A = 0 \qquad (11)$$

with

$$\begin{aligned} f_1 &= \langle \beta g^2 \rangle / c \\ f_2 &= -\frac{c_g - c}{c^2 k^2} \langle \beta g g_1 \rangle + 2\langle \lambda g g_1 \rangle - (2c_g + c)\langle \lambda g^2 \rangle \\ f_3 &= \frac{1}{2c^3} \langle g^2 g_2 \gamma \rangle - \frac{1}{c} \langle \beta \lambda g^2 \frac{\partial g_0}{\partial y} \rangle - \langle 2g \frac{\partial g}{\partial y} \lambda \mathcal{D}_0 g_0 \rangle \end{aligned}$$

The calculations are tedious, and details are relegated to Appendix A.

Solitary packet

Equation (11) is the nonlinear Schrödinger equation and has solitary solutions in which the packet dispersion is balanced by nonlinear steepening or flattening.

$$A = \mathcal{A}\,\mathrm{sech}(KX) e^{\imath \Omega T} \quad , \quad \Omega = k \frac{f_2}{f_1} K^2 \quad , \quad \mathcal{A}^2 = \frac{2 f_2}{f_3} K^2$$

with the condition that $f_2/f_3 > 0$. Fig. 7 shows K and Ω which determine the scale and change in propagation of the packet. We can regard the latter as a change in the carrier wave, which now looks like

$$A \exp(\imath k x - \imath \omega t + \imath \epsilon^2 \Omega t)$$

Since both $-\omega$ and Ω are positive, the carrier wave moves slightly faster to the west, while the packet is propagating to the east.

Larger amplitude waves will both be associated with a shorter packet and a larger speed-up of the carrier wave. Unlike the solitary Rossby waves in a channel (Malanotte-Rizzoli 1980) which exist for the long waves with westward group velocity (and in the regime where the carrier wave is unstable to modulational perturbations, Plumb, 1977), these travel in the opposite direction as the carrier wave. But, from the non-linear Schrödinger equation, modulation instability can indeed occur when $f_2/f_3 > 0$, so the isolated packets can form from an longer wave train.

DISCUSSION

We have shown that the topographic beta-effect can support either cyclonic solitons or, for topogra-

phies with $\partial^2(1/h^2)/\partial y^2$ negative, anticyclones. In the example, this topography has weak slope until near the outer boundary where it drops suddenly. However, the need for boundaries seems to make these solutions less useful than they might otherwise be.[3] A model with stratification, on the other hand, could lead to more relevant solutions; unlike the barotropic model here, the long waves with limited cross-topography structure can become nondispersive (Allen 1975), opening up the possibility of interesting solitary solutions, However, it is likely that the barotropic mode will be excited on flat areas, so that multiple scales will appear in y; we are currently studying this problem.

The nonlinear barotropic wave packets, on the other hand, have the nice feature that they can be confined over the topographic slope. Unlike beta-plane analogues, the group velocity is opposite in direction to the phase speed, This may depend on the specifics of the topography, which can, as we saw in the solitary wave discussion, change the sign of the group velocity. But for the topography with a limited region of slope joining flat regions, energy will be moving with the shallow region to its left (in the northern hemisphere), with the phase translating in the opposite direction.

Although we have used various topographic shapes, the qualitative results will not be terribly sensitive to the exact structure. There are two requirements for these nonlinear solutions to exist. First the linear problem ($\nabla \cdot \lambda \nabla \psi = \beta \psi / c$ with either just the cross-topographic derivatives for solitary waves or both for the groups) must have a well-behaved solution. Secondly, for solitary waves, the projection of the nonlinear terms on the lowest order cross-topographic structure must be non-zero. For groups, the requirement $f_1/f_2 > 0$ is more difficult to evaluate.

Nonlinearity will be important when the steepness $|\mathbf{u}|/c$ is not very small. Observations, (e.g., (Johns & Watts 1986)) suggest this ratio is indeed order one. It seems likely that the western boundary currents and associated eddies could provide a disturbance, but the solitary wave could be disrupted by encountering changes in the topographic slope or direction as well as by additional forcing before it really settles. However the calculations herein suggest that linear wave theory is only part of the story.

[3] Although a solution with just a boundary at the coast would be of interest.

ACKNOWLEDGMENTS

It is a pleasure to contribute to a volume honoring Affonso Mascarenhas. He was a student working with Prof. Mollo-Christensen, and I served on his thesis committee. His love for the ocean was obvious, as was his realization of oceanography's importance for Latin and South America. Comments by the reviewers and Margaret Gregory helped improve the paper.

REFERENCES

ABLOWITZ, M. & SEGUR, H. 1981. *Solitons and the inverse scattering transform*, Society for Industrial and Applied Mathematics, Philadelphia, 425p.

ALLEN, J. 1975. Coastal trapped waves in a stratified ocean, *J. Phys. Oceanogr.* 5, 300–325.

BAKER-YEBOAH, S., FLIERL, G., SUTYRIN, G. & ZHANG, Y. 2010. Transformation of an Agulhas eddy near the continental slope, *Ocean Science* 6, 143–159.

CLARKE, R. 1971. Solitary and cnoidal planetary waves, *Geophys. Fluid Dyn.* 2, 343–354.

FLIERL, G. & HAINES, K. 1994. The decay of modons due to Rossby wave radiation, *Phys. Fluids* 6, 3487–3497.

FLIERL, G., LARICHEV, V., MCWILLIAMS, J. & REZNIK, G. 1980. The dynamics of baroclinic and barotropic solitary eddies, *Dyn. of Atmos. and Oceans* 5, 1–41.

GARRETT, C. 1979. Topographic Rossby waves off east Australia: identification and role in shelf circulation, *J. Phys. Oceanogr.* 9, 244–253.

HAMILTON, P. 2009. Topographic Rossby waves in the Gulf of Mexico, *Prog. in Oceanogr.* 82, 1–31.

JOHNS, W. & WATTS, D. 1986. Time scales and structure of topographic Rossby waves and meanders in the deep Gulf Stream, *J. Mar. Res.* 44, 267–290.

LARICHEV, V. & REZNIK, G. 1976. Two-dimensional Rossby soliton: an exact solution, *Rep. U.S.S.R. Acad. Sci.* 231, 1077–1079.

LARSEN, L. 1965. Comments of "Solitary Waves in the Westerlies", *J. Atmos. Sci.* 22, 222–224.

LONG, R. 1964. Solitary waves in the westerlies, *J. Atmos. Sci.* 21, 197–200.

LOUIS, J., PETRIE, B. & SMITH, P. 1982. Observations of topographic Rossby waves on the continental margin off Nova Scotia, 12, 47–55.

MALANOTTE-RIZZOLI, P. 1980. Solitary Rossby waves over variable relief and their stability. Part II. Numerical experiments., *Dyn. Atmos. Oceans* 4, 261–294.

MALANOTTE-RIZZOLI, P. 1982. Planetary solitary waves in geophysical flows, *Advances in Geophysics* 24, 147–224.

MALANOTTE-RIZZOLI, P. & HENDERSHOTT, M. 1980. Solitary Rossby waves over variable relief and their stability. Part I. The analytical theory., *Dyn. Atmos. Oceans* 4, 247–260.

MOORE, D. & SAFFMAN, P. 1971. Structure of a line vortex in an imposed strain, *in* R. M. Olsen J.H., Goldburg A. (ed.), *Aircraft Wake Turbulence*, Plenum, New York, 339–353.

OEY, L. & LEE, H. 2002. Deep eddy energy and topographic Rossby waves in the Gulf of Mexico, *J. Phys. Oceanogr.* 32, 3499–3527.

PICKART, R. 1995. Gulf Stream-generated topographic Rossby waves, *J. Phys. Oceanogr.* 25, 574–86.

SHU, Y., XUE, H., WANG, D., CHAI, F., XIE, Q., CAI, S., CHEN, R., CHEN, J., LI, J. & HE, Y. 2016. Persistent and energetic bottom-trapped topographic Rossby waves observed in the southern South China Sea, *Scientific reports* 6(1), 1–8.

STERN, M. E. 1975. Minimal properties of planetary eddies, *J. Mar. Res.* 40, 57–74.

THOMPSON, R. 1971. Topographic Rossby waves at a site north of the Gulf Stream, *Deep Sea Res. and Oceanogr. Abstracts* 18, 1–19.

THOMPSON, R. & LUYTEN, J. 1976. Evidence for bottom-trapped topographic Rossby waves from single moorings, *Deep Sea Res. and Oceanogr. Abstracts* 23, 629–635.

WANG, Q., ZENG, L., SHU, Y., LI, J., CHEN, J., HE, Y., YAO, J.AND WANG, D. & ZHOU, W. 2019. Energetic topographic Rossby waves in the northern South China sea, *Jour. Phys. Oceanog.* 49(10), 2697–2714.

WANG, X. 1992. *Interaction of an Eddy with a Continental Slope*, PhD Thesis, MIT-WHOI.

YAMAGATA, T. 1980. On the nonlinear modulation of planetary topographic waves in a rotating stratified ocean, *Geophysical & Astrophysical Fluid Dynamics* 16(1), 35–54.

ZHANG, Y., PEDLOSKY, J. & FLIERL, G. 2011. Shelf circulation and cross-shelf transport out of a bay driven by eddies from an open-ocean current. Part I: Interaction between a barotropic vortex and a steplike topography, *J. Phys. Oceanogr.* 41, 889–910.

ZHAO, B. & TIMMERMANS, M. 2018. Topographic Rossby waves in the Arctic Ocean's Beaufort Gyre, *Journal of Geophysical Research: Oceans* 123(9), 6521–6530.

APPENDIX A: ALGEBRAIC DETAILS

Here, we give the term-by-term decomposition of the right-hand side of the second order equation (8)

$$\begin{aligned}\left[c\mathcal{L}_0-\beta\right]\psi_{2,x} &= -c\mathcal{L}_1\psi_{1,x}-c\mathcal{L}_2\psi_{0,x}-c_g\mathcal{L}_0\psi_{1,X}\\ &-c_g\mathcal{L}_1\psi_{0,X}+\beta\psi_{1,X}+\frac{1}{c}J_X(\psi_0\lambda\beta\psi_0)\\ &+\frac{1}{c}J(\psi_1,\lambda\beta\psi_0)+J(\psi_0,\lambda\mathcal{L}_0\psi_1)\\ &+J(\psi_0,\lambda\mathcal{L}_1\psi_0)+\frac{\beta}{c}\psi_{0,T}\end{aligned}$$

(with subscripts indication partial derivatives). We can split each term into the contribution to $e^{\imath kx}$ or the x-independent part. The former terms will be resonant and their sum, projected on $\exp(-\imath kx)g(y)$ gives the solvability condition, while the latter will determine A_0.

$$\begin{aligned}-c\mathcal{L}_1\psi_{1,x} &= \imath 2kA_{XX}\lambda g_1e^{\imath kx}\\ -c\mathcal{L}_2\psi_{0,x} &= -\imath kcA_{XX}\lambda ge^{\imath kx}\\ -c_g\mathcal{L}_0\psi_{1,X} &= -\imath\frac{c_g}{ck}A_{XX}\mathcal{D}_1g_1e^{\imath kx}-c_g|A|_X^2D_0g_0\\ -c_g\mathcal{L}_1\psi_{0,X} &= -2\imath kc_gA_{XX}\lambda ge^{\imath kx}\\ +\beta\psi_{1,X} &= \imath\frac{1}{ck}A_{XX}\beta g_1e^{\imath kx}+|A|_X^2\beta g_0\\ +\frac{1}{c}J_X(\psi_0\lambda\beta\psi_0) &= \frac{1}{c}|A|_X^2(\lambda\beta)_yg^2\\ +\frac{1}{c}J(\psi_1,\lambda\beta\psi_0) &= \frac{\imath k}{c}|A|^2A\left[\frac{1}{c^2}(\beta\lambda gg_2)_y-\beta\lambda gg_{0,y}\right]e^{\imath kx}\\ &\quad -\frac{1}{c^2}|A|_X^2(\beta\lambda gg_1)_y\\ +J(\psi_0,\lambda\mathcal{L}_0\psi_1) &= \frac{\imath k}{2c^2}|A|^2A\left[-g(\lambda D_2g_2)_y-2g_y\lambda D_2g_2\right.\\ &+ \left.2c^2g(\lambda D_0g_0)_y\right]e^{\imath kx}+\frac{1}{c}|A|_X^2(g\lambda\mathcal{D}_1g_1)_y\\ +J(\psi_0,\lambda\mathcal{L}_1\psi_0) &= 2k^2|A|_X^2(\lambda^2g^2)_y\\ \frac{\beta}{c}\psi_{0,T} &= \frac{1}{c}A_T\beta ge^{\imath kx}\end{aligned}$$

The zero mode terms are all proportional to $|A|_X^2$ and determine g_0

$$\begin{aligned}&-c_gD_0g_0+\beta g_0+\frac{\gamma}{c}g^2-\frac{1}{c^2}(\beta\lambda gg_1)_y\\ &+\frac{1}{c}(g\lambda\mathcal{D}_1g_1)_y+2k^2(\lambda^2g^2)_y=0\end{aligned}$$

Multiplying the $e^{\imath kx}$ terms by the adjoint and integrating leads to

$$A_T \frac{\langle \beta g^2 \rangle}{c} + \imath k A_{XX} \left[2\langle g\lambda g_1 \rangle - c\langle \lambda g^2 \rangle - \frac{c_g}{ck^2} \langle g\mathcal{D}_1 g_1 \rangle \right.$$
$$\left. - 2\langle \lambda g^2 \rangle + \frac{1}{ck^2} \langle \beta g g_1 \rangle \right] + \frac{\imath k}{c} |A|^2 A \left[\frac{1}{c^2} \langle g(\beta\lambda g g_2)_y \rangle \right.$$
$$-\langle \beta\lambda g g_{0,y} \rangle - \frac{1}{2c} \langle g^2 (\lambda\mathcal{D}_2 g_2)_y \rangle - \frac{1}{c} \langle g g_y \lambda\mathcal{D}_2 g_2 \rangle$$
$$\left. + c\langle g^2 (\lambda\mathcal{D}_0 g_0)_y \rangle \right] = 0$$

We can do a few integrations by parts (noting that $\langle \frac{\partial}{\partial y} F \rangle = 0$) and find

$$A_T \frac{\langle \beta g^2 \rangle}{c} + \imath k A_{XX} \left[2\langle g\lambda g_1 \rangle - c\langle \lambda g^2 \rangle - \frac{c_g}{c^2 k^2} \langle g\beta g_1 \rangle \right.$$
$$\left. -2c_g \langle \lambda g^2 \rangle + \frac{1}{ck^2} \langle \beta g g_1 \rangle \right] + \frac{\imath k}{c} |A|^2 A \left[\frac{1}{2c^2} \langle \gamma g^2 g_2 \rangle \right.$$
$$\left. -\langle \beta\lambda g^2 g_{0,y} \rangle - 2c\langle g g_y \lambda\mathcal{D}_0 g_0 \rangle \right] = 0$$

Expressing this as

$$f_1 A_T + \imath k f_2 A_{XX} + \imath k f_3 |A|^2 A = 0$$

gives the values of f_j in the text and leads to the sech solution.